Metasurface Design Using Electromagnetic Inversion

Trevor Brown[1], Chaitanya Narendra[1], Yousef Vahabzadeh[2], Christophe Caloz[2], and Puyan Mojabi[1]
[1]Department of Electrical and Computer Engineering, University of Manitoba, Winnipeg, MB, Canada
[2]Department of Electrical Engineering, École Polytechnique de Montréal, Montréal, QC, Canada

***Abstract*—This paper summarizes and synthetically evaluates a method proposed for metasurface design. The method takes as input a set of desired far-field (FF) performance specifications and produces an effective susceptibility distribution that, when illuminated with a known incident field, produces a FF radiation pattern exhibiting the desired specifications. To this end, electromagnetic inversion (inverse source) is used to solve for the desired tangential fields on the output side of the metasurface. A finite-difference frequency-domain solver, recently developed for simulation of metasurfaces, is used to synthetically evaluate the proposed method using a two-dimensional (2D) example. It should be noted that microscopic metasurface design (i.e., the design of the physical metasurface implementation) is beyond the scope of this paper.**

I. Introduction

The emergence of metamaterials in recent years offers a way to tailor the radiation produced by a source in a *controllable* way. In this work, we focus on (quasi) two-dimensional metamaterials, known as metasurfaces, which generally consist of a single thin layer of material constructed of subwavelength elements [1]. These elements and their interaction with local electromagnetic fields can be macroscopically described in terms of effective bianisotropic susceptibility tensors [2], although an equivalent formulation using effective surface impedances [3], [4], [5] is also common in the literature.

A metasurface is capable of implementing a desired electromagnetic discontinuity between two fields, as described by the generalized sheet transition conditions (GSTCs) [6]. Several design methods have been developed in recent years that allow for a transformation between an arbitrary incident field and arbitrary reflected and transmitted fields; however, these methods require the *explicit* (amplitude and phase) expressions of these desired fields (e.g., a refracted plane wave).

In [7], an inverse source algorithm was presented that offers more flexibility to the macroscopic design of metasurfaces: the ability to perform the design from a set of desired *performance specifications* for the transmitted field rather than its explicit expression. This approach can be more practical for antenna engineering applications as these performance specifications can be, for example, main beam directions, null directions, half-power beamwidth (HPBW), and polarization. Herein, given a set of performance specifications, we obtain surface susceptibilities of a metasurface using this inverse source approach, and then synthetically evaluate the metasurface performance using a finite-difference frequency-domain (FDFD) solver recently developed for metasurface simulation, which is referred to as FDFD-GSTC [8]. The physical implementation of the resulting surface susceptibility distributions (i.e., microscopic design [5]) is not within the scope of this paper.

II. Inverse Source Framework

The first part of the procedure is to find a field distribution on the metasurface boundary that produces a far-field (FF) pattern exhibiting the desired performance specifications. As described in [7], we use an inverse source technique to find a set of equivalent electric and magnetic currents ($\vec{J}$ and $\vec{M}$) on the metasurface boundary that produce a satisfactory FF pattern. These currents are found through the optimization of an appropriate cost functional using the conjugate gradient (CG) method. Enforcing Love's equivalence principle during the inversion process allows the desired transmitted fields, $\vec{E}^{\mathrm{t}}$ and $\vec{H}^{\mathrm{t}}$, to be calculated from the reconstructed currents as

$$\vec{E}^{\mathrm{t}} = \hat{n} \times \vec{M} \qquad \text{and} \qquad \vec{H}^{\mathrm{t}} = -\hat{n} \times \vec{J} \tag{1}$$

where $\hat{n}$ is the unit vector normal to the metasurface. Once the desired transmitted fields on the metasurface boundary are determined, the susceptibilities can be found by specifying the incident and reflected fields and using the procedure outlined in [2].

III. Illustrative Example

The example presented here is restricted to 2D for ease of simulation, but the general framework is applicable to 3D problems as presented in [7]. We consider the TE$_z$ polarization, where E_x, E_y, and H_z are the only nonzero field components. At a frequency of 1 GHz, the 1D metasurface located along the line $x = 0$ is 10λ in length, consisting of elements that are each of size $\lambda/50$. The desired FF specifications, shown in Table I, are enforced on a semicircular domain of radius 500λ with an angular resolution of $2°$. The reconstruction surface is chosen to be the metasurface boundary while Love's condition is enforced on the line $x = -\lambda/10$, at points uniformly spaced at $\lambda/75$ intervals. The equivalent currents J_y and M_z are found on the reconstruction surface using the inverse source algorithm [7], and the FF pattern produced by these currents is shown in Figure 1 (dashed curve). The desired transmitted fields are then calculated from the reconstructed currents via (1). Herein, the incident field is a 'tapered' plane wave which is normally incident and has a uniform amplitude of $H_z = 1\left[\mathrm{A/m}\right]$ for $|y| \leq 7\lambda$, and linearly tapers to zero

TABLE I
FAR-FIELD (FF) SPECIFICATIONS

Specifications	**Main Beam 1**	**Main Beam 2**
Direction	$\varphi = -30^\circ$	$\varphi = 20^\circ$
HPBW	20°	36°
Nulls (away from the main beam)	20°	30°

for $7\lambda < |y| \leq 10\lambda$. The desired transmitted fields are then scaled linearly such that the resulting metasurface elements are not active (a requirement of the simulation software). Since we are only dealing with TE_z case, the metasurface can be characterized with only four unknown susceptibility terms. As in [8], we stipulate that the susceptibilities corresponding to magnetoelectric coupling are zero for simplicity, resulting in

$$\chi_{\text{ee}}^{yy} = \frac{2}{j\omega\epsilon_0} \frac{H_z^{\text{i}} + H_z^{\text{r}} - H_z^{\text{t}}}{E_y^{\text{i}} + E_y^{\text{r}} + E_y^{\text{t}}} \quad \text{(2a)}$$

$$\chi_{\text{mm}}^{zz} = \frac{2}{j\omega\mu_0} \frac{E_y^{\text{i}} + E_y^{\text{r}} - E_y^{\text{t}}}{H_z^{\text{i}} + H_z^{\text{r}} + H_z^{\text{t}}} \quad \text{(2b)}$$

where χ_{ee}^{yy} and χ_{mm}^{zz} are the two remaining susceptibility terms and the i, r, and t superscripts denote the incident, reflected, and transmitted fields. Herein, we set the reflected fields to be zero, and solve for χ_{ee}^{yy} and χ_{mm}^{zz} given the incident fields and the transmitted fields found using the inverse source procedure. The field transformation using the computed susceptibilities is then simulated using the FDFD-GSTC solver [8]. The solution domain is of size 20λ by 30λ in the x and y dimensions, respectively. A perfectly matched layer is employed with a thickness of one wavelength on all sides of the domain. The resulting fields in the simulation domain are shown in Figure 2. The FF pattern is calculated by propagating the transmitted fields shown in Figure 2 to the FF region using a method-of-moments forward solver. The FF pattern corresponding to the simulated fields is shown in Figure 1 (solid curve), which is nearly identical to the FF pattern due to the equivalent currents (dashed curve) produced using the inversion algorithm. Lastly, the simulated FF pattern must be evaluated in terms of the original desired performance specifications. The main beams of the simulated FF pattern are in the $\varphi = -29^\circ$ and $\varphi = 21^\circ$ directions, with HPBWs of 18° and 35°, respectively. Nulls are also clearly present at $\varphi = -50^\circ$, $\varphi = -10^\circ$, and $\varphi = 50^\circ$, corresponding to the desired nulls at 20° and 30° away from the main beams. Comparing the observed metrics to the desired specifications in Table I, we can see that the desired specifications were satisfied with only a few minor deviations.

IV. CONCLUSION

We summarized a macroscopic metasurface design method that uses an inverse source framework with the goal of satisfying several FF performance specifications. A 2D illustrative example was presented and evaluated using an FDFD solver, with good agreement between the observed and desired FF metrics. Several practical challenges still remain, including the incorporation of constraints into the inversion process such that the resulting metasurface is passive and lossless, which will be discussed along with other topics such as non-existence and non-uniqueness of the solution at the conference.

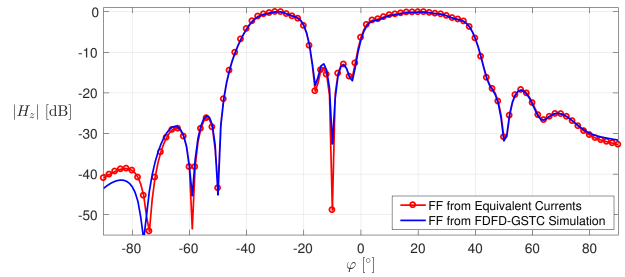

Fig. 1. A comparison of the normalized FF pattern produced by the equivalent currents (dashed red curve) and the normalized FF pattern resulting from the FDFD-GSTC simulation of the corresponding metasurface (solid blue curve).

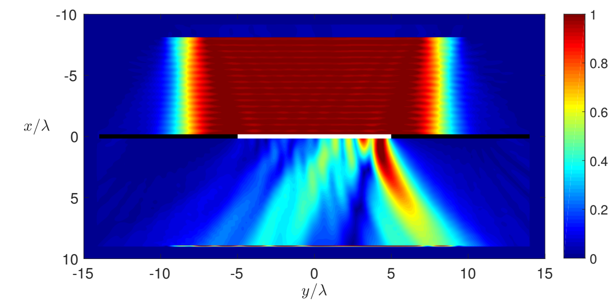

Fig. 2. Fields resulting from the FDFD-GSTC simulation of the metasurface designed using the inverse source method when illuminated with a normally incident plane wave. (The designed metasurface is at $x = 0$ for $-5\lambda \leq y \leq 5\lambda$, as shown by the solid white line. Absorbing susceptibilities have been used along $x = 0$ for $|y| > 5\lambda$, as indicated by the solid black lines.)

REFERENCES

[1] C. L. Holloway, E. F. Kuester, J. A. Gordon, J. O'Hara, J. Booth, and D. R. Smith, "An overview of the theory and applications of metasurfaces: The two-dimensional equivalents of metamaterials," *IEEE Antennas and Propagation Magazine*, vol. 54, no. 2, pp. 10–35, 2012.

[2] K. Achouri, M. A. Salem, and C. Caloz, "General metasurface synthesis based on susceptibility tensors," *IEEE Transactions on Antennas and Propagation*, vol. 63, no. 7, pp. 2977–2991, 2015.

[3] A. Grbic, R. Merlin, E. M. Thomas, and M. F. Imani, "Near-field plates: Metamaterial surfaces/arrays for subwavelength focusing and probing," *Proceedings of the IEEE*, vol. 99, no. 10, pp. 1806–1815, 2011.

[4] S. Tretyakov, "Metasurfaces for general transformations of electromagnetic fields," *Philos. Trans. Royal Soc. A: Mathematical, Physical and Engineering Sciences*, vol. 373, no. 2049, p. 20140362, 2015.

[5] A. Epstein and G. V. Eleftheriades, "Huygens' metasurfaces via the equivalence principle: design and applications," *JOSA B*, vol. 33, no. 2, pp. A31–A50, 2016.

[6] E. F. Kuester, M. A. Mohamed, M. Piket-May, and C. L. Holloway, "Averaged transition conditions for electromagnetic fields at a metafilm," *IEEE Transactions on Antennas and Propagation*, vol. 51, no. 10, pp. 2641–2651, 2003.

[7] T. Brown, C. Narendra, and P. Mojabi, "On the use of the source reconstruction method for metasurface design," 12^{th} *European Conference on Antennas and Propagation (EuCAP 2018)*, pp. 302–306, April 2018.

[8] Y. Vahabzadeh, K. Achouri, and C. Caloz, "Simulation of metasurfaces in finite difference techniques," *IEEE Trans. Antennas Propag*, vol. 64, no. 11, pp. 4753–4759, 2016.